Compartment Model of Low Earth Orbit System and Simulations of their Stochastic Interactions

Jaewon Choi, Purdue Summer Graduate Intern 2024

1 Introduction

The dynamics of derelicts, satellites, and debris in space are influenced by various factors such as collisions, satellite failures, and atmospheric drag, which can lead to unpredictable and complex interactions over time. In this report, we aim to model these interactions using a compartmental approach that divides the population into: derelicts, satellites, and debris. Each compartment represents the population size of the corresponding type at a given time. The interactions between these groups, such as collisions and drag, lead to transitions between states, which can be modeled using deterministic and stochastic approaches. We derive Ordinary Differential Equations (ODEs) and compare the results to JASON model (Long et al., 2020) and MOCAT model (D'Ambrosio et al., 2022; D'Ambrosio et al., 2023). Then we derive Stochastic Differential Equations (SDEs) and compare the deterministic and stochastic aspects of population dynamics through simulations.

2 Compartment Model

In the context of Low Earth Orbit (LEO), we model the population dynamics of different species through compartment model. Anthropogenic space objects can be divided into qualitatively distinct species:

- Satellites (S) are active, functioning objects.
- Derelicts (D) are non-functional satellites.
- Debris (N) is the collection of fragments produced by collisions.

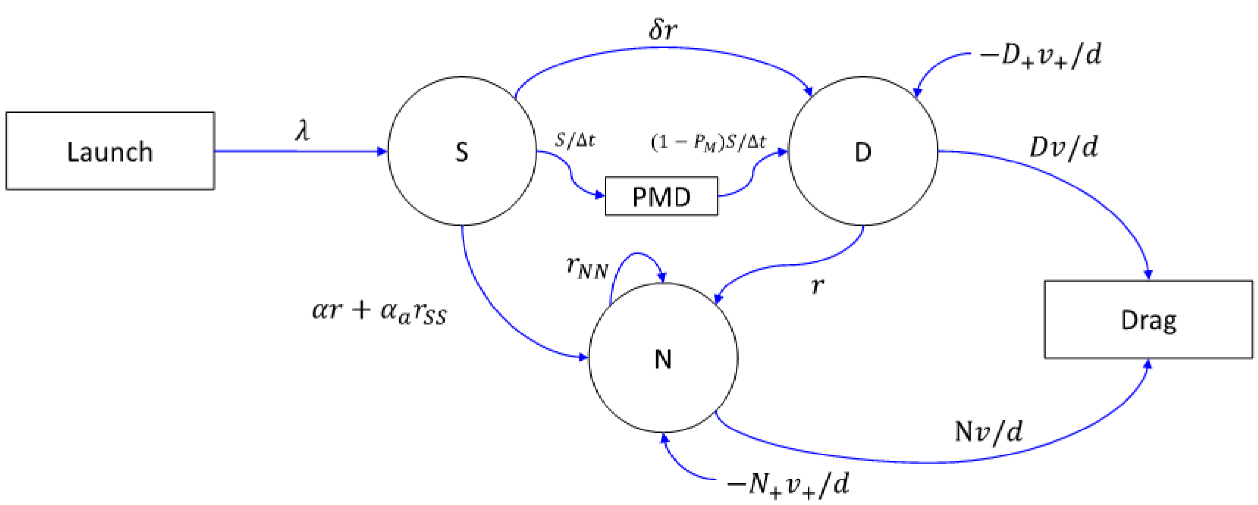

Figure 1: Compartment model of LEO system

The primary interactions in the system involve collisions between these objects, leading to the creation of debris and derelicts. Atmospheric drag and new satellite launches serve as removal and generation processes, respectively, forming a source-sink system. We use a compartment modeling scheme shown in Figure 1 to track the transitions between these states over time. The following sections describe the process of formulating the system as a Markov jump process, approximating to ordinary differential equations (ODEs), and refining with stochastic differential equations (SDEs).

3 Markov Jump Process and Ordinary Differential Equations

A compartment model is commonly described by a system of Ordinary Differential Equations (ODEs), which model the average, deterministic evolution of populations in each compartment over time. These equations are derived from the transition rates between compartments and provide implications on the long-term trends in the system.

We first formulate the LEO system as a Markov jump process(MJP). This MJP captures the exact transitions between discrete states caused by collisions. We then approximate the MJP using ODEs to describe the deterministic, average behavior of the system. The ODE suggests that when the volume of each shell is large and the system propagates over a long time horizon, the random fluctuations from individual collisions tend to average out. The ODE approximation provides a smooth, continuous representation of the system's behavior by focusing on the expected rate of change in the population. The following subsections describe the dynamics of each species by Markov jump process then derive the ODEs related to collisions.

3.1 Derelict Dynamics

In this subsection, we specifically model the probability of changes in the population dynamics of derelicts, denoted $\hat{X}_{V,D}(t)$, due to collisions through Markov jump process and derive the long-term average dynamics through a system of ODEs.

The probability of a decrease in the derelict population due to a derelict-debris or derelict-satellite collision is given by:

$$
\begin{aligned}
&P(\hat{X}_{V,D}(t+h) = D-1 | \hat{X}_V(t) = (S,D,N)) = \\
&\qquad \binom{D}{1}\left(\sigma_{DN} v \frac{N}{V} h\right)^1 \left(1 - \sigma_{DN} v \frac{N}{V} h\right)^{D-1} \\
&\qquad + \binom{D}{1}\left(\alpha\sigma_{DS} v \frac{S}{V} h\right)^1 \left(1 - \alpha\sigma_{DS} v \frac{S}{V} h\right)^{D-1} \\
&\qquad + (\frac{v}{d} D h + o(h)) \\
&\qquad = Vh\left(\sigma_{DN} v \frac{N}{V}\frac{D}{V} + \alpha\sigma_{DN} v \frac{S}{V}\frac{D}{V}\right) + \frac{v}{d} D h + o(h)
\end{aligned}
$$

$\hat{X}_{V,D}(t)$ represents the number of derelicts at time t. $P(\hat{X}_{V,D}(t+h) = D-1|\hat{X}_{V,D}(t) = D)$ is the probability that one individual of derelict is removed from the population due to a collision with either debris or a satellite. σ_{ij} represents the square of the impact parameter and it is a function of the radius of the colliding objects, $\sigma_{ij} = (r_i + r_j)^2$, where i, j are the subscripts indicating each species. N and S represent the number of debris and satellites, and v is the average relative velocity, while V is the volume of a shell. α is the fraction of collision with derelict or debris that an active satellite fails to avoid. We can extend this model to include the effect of atmospheric drag on the derelict population, treating it as a Poisson process with rate $\frac{v}{d}D$ where v is the change in semimajor axis, d is the thickness of shell, and D is the number of derelict species in current shell at time t. Drag effect is modeled as an exponential clock associated with each object, triggering the removal of derelicts from orbit.

The probability of an increase in the derelict population is given by:

$$
\begin{aligned}
&P(\hat{X}_{V,D}(t+h) = D+1|\hat{X}_V(t) = (S,D,N)) = \\
&\qquad \binom{S}{1}\left(\delta\sigma_{SN}v\frac{N}{V}h\right)^1\left(1-\delta\sigma_{SN}v\frac{N}{V}h\right)^{S-1} \\
&\qquad +\binom{S}{1}\left(\delta\sigma_{DS}v\frac{D}{V}h\right)^1\left(1-\delta\sigma_{DS}v\frac{D}{V}h\right)^{S-1} \\
&\qquad +(\frac{v_+}{d_+}D_+h + o(h)) \\
&\qquad = Vh\left(\delta\sigma_{SN}v\frac{N}{V}\frac{S}{V} + \delta\sigma_{DS}v\frac{D}{V}\frac{S}{V}\right) + \frac{v_+}{d_+}D_+h + o(h)
\end{aligned}
$$

Here, $P(\hat{X}_{V,D}(t+h) = D+1 \mid \hat{X}_V(t) = (S,D,N))$ represents the probability of the derelict population increasing due to degenerating interactions between satellites and debris or between satellites and derelicts. δ is the ratio of the density of disabling to lethal debris. This parameter implies that some collisions involving satellites are lethal, creating debris, while some collisions result in degenerating satellites into derelicts. Atmospheric drag can also increase the derelict population. Derelicts coming from the upper shell can be modeled as a Poisson process with rate $\frac{v_+}{d_+}D_+$ where the subscript + refers to the quantities related to the upper shell.

Finally, for a derelict-derelict collision that decreases the population by 2 is represented by:

$$
\begin{aligned}
&P(\hat{X}_{V,D}(t+h) = D-2|\hat{X}_V(t) = (S,D,N)) = \\
&\qquad \binom{D}{1}\left(\sigma_{DD}v\frac{D}{V}h\right)^1\left(1-\sigma_{DD}v\frac{D}{V}h\right)^{D-1} \\
&\qquad = Vh\left(\sigma_{DD}v\frac{D}{V}\frac{D}{V}\right) + o(h)
\end{aligned}
$$

The collision between two derelicts removes two derelict individuals from the population. Therefore, this can be modeled by a jump size of 2.

From these probabilistic models, we derive the Ordinary Differential Equation (ODE) that describes the rate of change of the derelict population over time. We begin with modeling a stochastic process of $\hat{X}_{V,D}(t)$, the derelict population at time t:

$$
\hat{X}_{V,D}(t) = \hat{X}_{V,D}(0) + \sum_{i=1}^{k} e_i N_i\left(\int_0^t V\lambda_i\left(\frac{\hat{X}_V(u)}{V}\right)du\right)
$$

This equation represents the stochastic evolution of the derelict population over time, taking into account various interactions, where $e_i \in \{-2,-1,+1\}$ is the jump size with corresponding transition rate $\lambda_i\left(\frac{\hat{X}_V(u)}{V}\right)$, $\hat{X}_V = (\hat{X}_{V,S}, \hat{X}_{V,D}, \hat{X}_{V,N})$, and N_i is the unit-rate Poisson process. The integral $\int_0^t V\lambda_i\left(\frac{\hat{X}_V(u)}{V}\right)du$ represents the cumulative rate of collisions up to time t. The interaction rates are normalized by the volume V.

If we let $x_D : \mathbb{R}_+ \to \mathbb{R}^b$, and $x = (x_S, x_D, x_N)$ be the solution to the integral equation:

$$
x_D(t) = x_D(0) + \int_0^t F(x(s))ds
$$

where $F(x) := \sum_{i=1}^{k} e_i\lambda_i(x)$,

jump direction e_i and corresponding function $\lambda_i : \mathbb{R}^d \to \mathbb{R}_+$

then for the process $(\hat{X}_V(t))_{t\in\mathbb{R}}$:

$$\hat{X}_V(t) = \hat{X}_V(0) + \sum_{i=1}^{k} e_i N_i \left(\int_0^t V\lambda_i \left(\frac{\hat{X}_V(u)}{V} \right) du \right),$$

$$\lim_{V\to\infty} \sup_{0\le t\le T} \left| \frac{1}{V} X_V(t) - x(t) \right| = 0 \quad a.s.$$

for sufficiently large V (Kurtz's theorem, Ethier and Kurtz (2009)).

According to Draief and Massoulié (2009), population density $X_V(t) = \frac{1}{V}\hat{X}_V(t)$ can be approximated by $x(t)$, and thus the population $\hat{X}_V(t)$ can be approximated by $\hat{x}(t)$

$$\begin{aligned}
\frac{dx_D}{dt} &= -1 \times \left(\sigma_{DN} v x_D x_N + \alpha\sigma_{DS} v x_D x_S + \frac{v}{d} x_D \right) \\
&\quad + 1 \times \left(\delta\sigma_{SN} v x_S x_N + \delta\sigma_{SD} v x_S x_D + \frac{v_+}{d_+} x_{+D} \right) \\
&\quad - 2 \times (\sigma_{DD} v x_D x_V) \\
&= -\sigma_{DN} v x_D x_N - \alpha\sigma_{DS} v x_D x_S + \delta\sigma_{DS} v x_S x_D + \delta\sigma_{NS} v x_S x_N - 2\sigma_{DD} v x_D x_D - \frac{v}{d} x_D + \frac{v_+}{d_+} x_{+D}
\end{aligned}$$

, and

$$\begin{aligned}
\frac{d\hat{x}_D}{dt} &= -1 \times V \left(\sigma_{DN} v \frac{\hat{x}_D}{V}\frac{\hat{x}_N}{V} + \alpha\sigma_{DS} v \frac{\hat{x}_D}{V}\frac{\hat{x}_S}{V} + \frac{v}{d}\frac{\hat{x}_D}{V} \right) \\
&\quad + 1 \times V \left(\delta\sigma_{SN} v \frac{\hat{x}_S}{V}\frac{\hat{x}_N}{V} + \delta\sigma_{SD} v \frac{\hat{x}_S}{V}\frac{\hat{x}_D}{V} + \frac{v_+}{d_+}\frac{\hat{x}_{+D}}{V} \right) \\
&\quad - 2 \times V \left(\sigma_{DD} v \frac{\hat{x}_D}{V}\frac{\hat{x}_D}{V} \right) \\
&= -\frac{\sigma_{DN} v}{V} \hat{x}_D \hat{x}_N - \alpha \frac{\sigma_{DS} v}{V} \hat{x}_D \hat{x}_S + \delta \frac{\sigma_{DS} v}{V} \hat{x}_S \hat{x}_D + \delta \frac{\sigma_{NS} v}{V} \hat{x}_S \hat{x}_N - 2 \frac{\sigma_{DD} v}{V} \hat{x}_D \hat{x}_D - \frac{v}{d} \hat{x}_D + \frac{v_+}{d_+} \hat{x}_{+D}
\end{aligned}$$

follows. This ODE differs from the MOCAT model since it considers the removal of a derelict due to derelict-satellite collision, denoted by $-\alpha\sigma_{DS} v x_D x_S$, and the removal of two derelict species due to derelict-derelict collision, $-2\sigma_{DD} v x_D x_D$, while the MOCAT model only counts one.

3.2 Satellite Dynamics

The probability of a decrease in the satellite population, denoted as $\hat{X}_S(t)$, is given by:

$$\begin{aligned}
&P(\hat{X}_{V,S}(t+h) = S-1 | \hat{X}_V(t) = (S, D, N)) = \\
&\qquad \binom{S}{1} \left(\delta\sigma_{NS} v \frac{N}{V} h \right)^1 \left(1 - \delta\sigma_{NS} v \frac{N}{V} h \right)^{S-1} \\
&\qquad + \binom{S}{1} \left(\delta\sigma_{DS} v \frac{D}{V} h \right)^1 \left(1 - \delta\sigma_{DS} v \frac{D}{V} h \right)^{S-1} \\
&\qquad + \binom{S}{1} \left(\alpha\sigma_{NS} v \frac{N}{V} h \right)^1 \left(1 - \alpha\sigma_{NS} v \frac{N}{V} h \right)^{S-1} \\
&\qquad + \binom{S}{1} \left(\alpha\sigma_{DS} v \frac{D}{V} h \right)^1 \left(1 - \alpha\sigma_{DS} v \frac{D}{V} h \right)^{S-1} \\
&\qquad = Vh((\delta+\alpha)\sigma_{NS} v \frac{N}{V}\frac{S}{V} + (\delta+\alpha)\sigma_{DS} v \frac{D}{V}\frac{S}{V}) + o(h)
\end{aligned}$$

$P(\hat{X}_{V,S}(t+h) = S-1|\hat{X}_{V,S}(t) = S)$ is the probability of the satellite population decreasing by 1 due to a lethal or degenerating collision with debris or derelicts. α is the fraction of lethal collision with derelict or debris that an active satellite fails to avoid, and δ is the ratio of the density of disabling to lethal debris. N and D represent the populations of debris and derelicts, and S is the number of satellites.

For satellite-satellite collisions that decrease the population by 2:

$$\begin{aligned} P(\hat{X}_{V,S}(t+h) = S-2|\hat{X}_V(t) = (S,D,N)) = \\ \binom{S}{1}\left(\alpha_a \sigma_{SS} v \frac{S}{V} h\right)^1 \left(1 - \alpha_a \sigma_{SS} v \frac{S}{V} h\right)^{S-1} \\ = Vh\left(\alpha_a \sigma_{SS} v \frac{S}{V}\frac{S}{V}\right) + o(h) \end{aligned}$$

This equation represents the probability of two satellites colliding, which removes two satellites from the population. α_a is the fraction of collisions among satellites that an active satellite fails to avoid. This differs from the MOCAT model which considers only one satellite to be removed from the system.

The satellite population can increase by launch. We can model the launch events as a Poisson process to describe each individual launcher having a small probability of launching a satellite in any small time interval. Suppose λ is the aggregate launch rate per unit volume across all launchers. Given the Poisson process, the probability that the satellite population increases by 1 in the interval h due to a launch is:

$$P(\hat{X}_S(t+h) = S+1|\hat{X}_V(t) = (S,D,N)) = V\lambda + o(h)$$

This equation implies that in any small time interval h there is a chance proportional to $V\lambda h$ that a satellite will be launched.

The corresponding differential equation governing the satellite population density is:

$$\begin{aligned} \frac{dx_S}{dt} &= \lambda - 1 \times ((\delta+\alpha)\sigma_{NS} v x_N x_S + (\delta+\alpha)\sigma_{DS} v x_D x_S) \\ &\quad - 2 \times (\alpha_a \sigma_{SS} v x_S x_S) \\ &= -(\delta+\alpha)\sigma_{NS} v x_N x_S - (\delta+\alpha)\sigma_{DS} v x_D x_S - 2\alpha_a \sigma_{SS} v x_S x_S \end{aligned}$$

This differential equation describes how the satellite population density changes over time, considering launches, satellite-debris/derelict interactions, and satellite-satellite collisions. The first term represents the decrease in satellite population due to collisions with debris and derelicts. The second term models the decrease due to catastrophic satellite-satellite collisions.

3.3 Debris Dynamics

The debris population dynamics, denoted $\hat{X}_N(t)$, involve both catastrophic(S/D - S/D) and non-catastrophic(N-S/D/N) collisions. The jump sizes in the debris dynamics reflect the number of fragments generated due to each type of collision. The equations representing the jump sizes are:

$$\begin{aligned} n_{f,c} &= 0.1 L_C^{-1.71} (M_i + M_j)^{0.75} \\ n_{f,nc} &= 0.1 L_C^{-1.71} (M_p \dot{v}_{imp}^2)^{0.75} \end{aligned}$$

where L_C is the characteristic length of the minimum size of generated debris, $M_{i/j}$ is the mass associated to the species i, j, $M_p = \min(M_i, M_j)$, and v_{imp} is the impact velocity (10 km/s).

For catastrophic collisions that increase the debris population, we have:

$$
\begin{aligned}
P(\hat{X}_{V,N}(t+h) = N + n_{f,c} | \hat{X}_V(t) = (S,D,N)) = & \\
& + \binom{S}{1}\left(\alpha\sigma_{DS}v\frac{D}{V}h\right)^1\left(1-\alpha\sigma_{DS}v\frac{D}{V}h\right)^{S-1} \\
& + \binom{S}{1}\left(\alpha_a\sigma_{SS}v\frac{S}{V}h\right)^1\left(1-\alpha_a\sigma_{SS}v\frac{S}{V}h\right)^{S-1} \\
& + \binom{D}{1}\left(\sigma_{DD}v\frac{D}{V}h\right)^1\left(1-\sigma_{DD}v\frac{D}{V}h\right)^{D-1} \\
& = Vh(\alpha\sigma_{DS}v\frac{D}{V}\frac{S}{V} + \alpha_a\sigma_{SS}v\frac{S}{V}\frac{S}{V} + \sigma_{DD}v\frac{D}{V}\frac{D}{V}) + o(h)
\end{aligned}
$$

Non-catastrophic collision dynamics can be expressed as:

$$
\begin{aligned}
P(\hat{X}_{V,N}(t+h) = N + n_{f,nc} | \hat{X}_V(t) = (S,D,N)) = & \\
& + \binom{D}{1}\left(\sigma_{DN}v\frac{N}{V}h\right)^1\left(1-\sigma_{DN}v\frac{N}{V}h\right)^{D-1} \\
& + \binom{S}{1}\left(\alpha\sigma_{SN}v\frac{N}{V}h\right)^1\left(1-\alpha\sigma_{SN}v\frac{N}{V}h\right)^{S-1} \\
& + \binom{N}{1}\left(\sigma_{NN}v\frac{N}{V}h\right)^1\left(1-\sigma_{NN}v\frac{N}{V}h\right)^{N-1} \\
& = Vh(\sigma_{DN}v\frac{D}{V}\frac{N}{V} + \alpha\sigma_{SN}v\frac{S}{V}\frac{N}{V} + \sigma_{NN}v\frac{N}{V}\frac{N}{V}) + o(h)
\end{aligned}
$$

The debris species are also subject to atmospheric drag. The drag dynamics can be expressed as:

$$
\begin{aligned}
P(\hat{X}_{V,N}(t+h) = N - 1 | \hat{X}_V(t) = (S,D,N)) &= \frac{v}{d}Nh + o(h) \\
P(\hat{X}_{V,N}(t+h) = N + 1 | \hat{X}_V(t) = (S,D,N)) &= \frac{v_+}{d_+}N_+h + o(h)
\end{aligned}
$$

The corresponding ODE for debris population density is:

$$
\begin{aligned}
\frac{dx_N}{dt} =& n_{f,nc}\left(\sigma_{DN}vx_Dx_N + \alpha\sigma_{NS}vx_Nx_S + \sigma_{NN}vx_Nx_N\right) + \frac{v}{d}x_Nh \\
&+ n_{f,c}\left(\alpha\sigma_{DS}vx_Dx_S + \alpha_a\sigma_{SS}vx_Sx_S + \sigma_{DD}vx_Dx_D\right) + \frac{v_+}{d_+}x_{+N}h
\end{aligned}
$$

The first term models non-catastrophic interactions, while the second term models catastrophic events that significantly increase the debris population.

4 Stochastic Differential Equations

This section describes the compartment model through stochastic differential equations (SDEs). Particularly, we begin by approximating the population dynamics of each species in the LEO system due to the interactions at a given volume at a given time.

4.1 Population Dynamics due to Interactions

We model the population dynamics of a generic species Q in a given volume V at time t. The population density $X_{V,Q}(t)$ of species Q in volume V is defined as:

$$
X_{V,Q}(t) = \frac{\hat{X}_{V,Q}(t)}{V}
$$

Here:

- $\hat{X}_{V,Q}(t)$ is the total number of species Q at time t within volume V.
- $X_{V,Q}(t)$ represents the number density of species Q, i.e. the population of the species is per unit volume at time t.

The stochastic dynamics of the population of species Q are given by the following equation:

$$\hat{X}_{V,Q}(t) = \hat{X}_{V,Q}(0) + \sum_{\ell} \ell \cdot Y_{\ell,Q}\left(V \int_0^t \beta_{\ell,Q}\left(\frac{\hat{X}_V(t)}{V}\right) du\right)$$

In this equation, $\hat{X}_{V,Q}(0)$ is the initial population of species Q at time $t = 0$. The summation $\sum_{\ell} \ell \cdot Y_{\ell,Q}$ represents the cumulative effect of all possible interaction events that lead to changes in the population of species Q. Each interaction results in a change of population by a jump size of ℓ. $Y_{\ell,Q}$ represents independent Poisson processes. It models the collision affecting the population, where $\beta_{\ell,Q}(X)$ is the rate of collision. Thus, this equation models how the population evolves over time, incorporating the initial population and random jumps due to interaction events.

Next, we define $F_Q(X)$:

$$F_Q(X) = \sum_{\ell} \ell \beta_{\ell,Q}(X)$$

This function $F_Q(X)$ represents the net change in the population caused by the interactions. Specifically, ℓ represents the jump size (e.g., an increase or decrease in population), and $\beta_{\ell,Q}(X)$ is the rate at which this event occurs.

Now, we can express the population dynamics of $X_{V,Q}(t)$:

$$X_{V,Q}(t) = X_{V,Q}(0) + \sum_{\ell} \frac{1}{V} \tilde{Y}_{\ell,Q}\left(V \int_0^t \beta_{\ell,Q}(X_V(u)) du\right) + \int_0^t F_Q(X_V(u)) du$$

where $X_{V,Q}(0)$ is the initial population density at $t = 0$, $\tilde{Y}_{\ell,Q}(u) = Y_{\ell,Q}(u) - u$ is the Poisson process centered at its expectation, and it is scaled by $\frac{1}{V}$ to account for the volume.

4.2 Pre-limit and Limit Equations

As the volume scales at a same rate, the system tends toward a deterministic limit. The pre-limit equation is:

$$X_{V,Q}(t) = X_{V,Q}(0) + \sum_{\ell} \frac{1}{V} \tilde{Y}_{\ell,Q}\left(V \int_0^t \beta_{\ell,Q}(X_V(u)) du\right) + \int_0^t F_Q(X_V(u)) du$$

Suppose that X_Q satisfies:

$$X_Q(t) = x_0 + \int_0^t F_Q(X(u)) du$$

Then for every $t \geq 0$,

$$\lim_{V \to \infty} P\left(\sup_{0 \leq s \leq t} |X_{V,Q}(s) - X_Q(s)| > \epsilon\right) = 0$$

This indicates that the stochastic process $X_{V,Q}(t)$ converges to the deterministic solution $X_Q(t)$ almost surely as the volume increases.

4.3 Scaling and Approximation

We now introduce a scaled process $H_{V,Q}(t)$, which measures the deviation of the stochastic process from the deterministic limit:

$$H_{V,Q}(t) = \sqrt{V}(X_{V,Q}(t) - X_Q(t))$$

$H_{V,Q}(t)$ represents the fluctuations of the population dynamics around the deterministic limit, scaled by $\sqrt{V}$. The scaled process $H_{V,Q}(t)$ satisfies the following stochastic differential equation (SDE):

$$H_{V,Q}(t) = H_{V,Q}(0) + \sum_{\ell} \ell W_{\ell,Q}^{(V)} \left(\int_0^t \beta_{\ell,Q}(X_V(u))du \right) + \int_0^t \sqrt{V}(F_Q(X_V(u)) - F_Q(X(u)))du$$

Where: $W_{\ell,Q}^{(V)} = 1/\sqrt{V}\tilde{Y}_{\ell,Q}(Vu)$ is a scaled Poisson process, which converges to a Brownian motion $W_{\ell,Q}$ as $V \to \infty$. The second term represents the deterministic drift, scaled by $\sqrt{V}$, which quantifies the difference between the stochastic and deterministic drift terms.

If we set $X_{V,Q} = X_Q + 1/\sqrt{V}H_{V,Q}$, $H_Q(t)$, which is the limit of $H_{V,Q}$, satisfies:

$$H_Q(t) = H_Q(0) + \sum_{\ell} \ell W_{\ell,Q} \left(\int_0^t \beta_{\ell,Q}(X_V(u))du \right) + \int_0^t \partial F_Q(X(u))^T H_Q(u)du$$

This equation describes the evolution of the deviations from the deterministic limit, driven by both stochastic and deterministic terms.

4.4 Approximation of $X_{V,Q}(t)$

Finally, we can approximate the population dynamics $X_{V,Q}(t)$ through $\tilde{Z}_{V,Q} = X_Q + \frac{1}{\sqrt{V}}H_Q$. If we substitute X_Q and H_Q, we can get the following equation:

$$\begin{aligned}\tilde{Z}_{V,Q}(t) &= X_Q(0) + \frac{1}{\sqrt{V}}H_Q(0) + \frac{1}{\sqrt{V}}\sum_{\ell} \ell \int_0^t \beta_{\ell,Q}^{1/2}(X(u))dW_{\ell,Q}(u) \\ &+ \int_0^t \left(F_Q(X(u)) + \partial F_Q(X(u))(\tilde{Z}_{V,Q}(u) - X_Q(u)) \right) du\end{aligned}$$

Here, $W_\ell \left(\int_0^t \beta_\ell(X(u))du \right) \to \int_0^t \beta_\ell^{1/2}(X(u))dW_\ell(u)$ can be shown through quadratic variations.

An equivalent approximation is as follows:

$$Z_{V,Q}(t) = X_Q(0) + \frac{1}{\sqrt{V}}\sum_{\ell} \ell \int_0^t \beta_{\ell,Q}^{1/2}(X(u))dW_{\ell,Q}(u) + \int_0^t F_Q(X(u))du$$

Theorem 3.2 of Ethier and Kurtz (2009) states that $\tilde{Z}_{V,Q}(t)$ and $Z_{V,Q}(t)$ are asymptotically equivalent.

4.5 Atmospheric Drag and Launch

We now add the terms related to atmospheric drag and launch to the existing SDEs. To formulate the drag effect, each object from species subject to drag, i.e. derelict and debris, is modeled as having an exponential clock that triggers atmospheric drag. Then the occurrence of drag follows a Poisson process with the rate denoted by β_{drag}. We can describe the evolution of species $Q \in \{D, N\}$ considering collisions and drag as:

$$\begin{aligned}X_{V,Q}(t) &= X_{V,Q}(0) + \sum_{\ell} \frac{1}{V} \ell Y_{\ell,Q} \left(V \int_0^t \beta_{\ell,Q}(X_V(u))du \right) \\ &- \frac{1}{V} Y_{\text{drag}}^{+} \left(V \int_0^t \beta_{\text{drag},Q}^{+}(X_{V,Q}(u))du \right) + \frac{1}{V} Y_{\text{drag}}^{-} \left(V \int_0^t \beta_{\text{drag},Q}^{-}(X_{V,Q}(u))du \right)\end{aligned}$$

Here, $\beta_{\text{drag},Q}(x) = \frac{v}{d}x$ is the rate of atmospheric drag for species Q, with d is the thickness of the shells and v is related to the change in semi-major axis. The superscript $+$ refers to the quantities related to the upper shell and superscript - refers to quantities related to current shell.

When $V \to \infty$, the limiting equation for species Q is:

$$X_Q(t) = X_Q(0) + \int_0^t F_Q(X(u))du - \int_0^t \beta^+_{\text{drag},Q}(X_Q(u))du + \int_0^t \beta^-_{\text{drag},Q}(X_Q(u))du$$

where $F_Q(X) = \sum_\ell \ell\beta_{\ell,Q}(X)$ is the deterministic change due to collisions and $\beta_{\text{drag},Q}(X_Q(u))$ is the change of species due to atmospheric drag.

The next step involves approximating the difference between the stochastic dynamics and the deterministic limit. Similar to section 4.3, we define $H_{V,Q}(t) = \sqrt{V}(X_{V,Q}(t) - X_Q(t))$ which represents the scaled deviation from the deterministic limit. Then the limit process for this deviation is:

$$\begin{aligned}
H_Q(t) = H_Q(0) &+ \sum_\ell \ell W_{\ell,Q}\left(\int_0^t \beta_{\ell,Q}(X(u))du\right) \\
&- W_{drag,Q}\left(\int_0^t \beta^+_{drag,Q}(X_Q(u))du\right) + W_{drag,Q}\left(\int_0^t \beta^-_{drag,Q}(X_Q(u))du\right) \\
&- \int_0^t \left(\partial F_Q(X(u)) - \partial\beta^+_{\text{drag},Q}(X_Q(u)) + \partial\beta^-_{\text{drag},Q}(X_Q(u))\right) H_Q(u)du
\end{aligned}$$

where $W^{(V)}_{\ell,Q}(u) = \frac{1}{\sqrt{V}}\tilde{Y}_{\ell,Q}(Vu)$, $W^{(V)}_{drag,Q}(u) = \frac{1}{\sqrt{V}}\tilde{Y}_{drag,Q}(Vu)$ are Brownian motions representing the random fluctuations in the collision and drag processes, and $W^{(V)}_{\ell,Q}(u) \to W_{\ell,Q}$, $W^{(V)}_{drag,Q}(u) \to W_{drag,Q}$, respectively.

Then we can approximate the population dynamics $X_{V,Q}(t)$ considering both the collision and drag through:

$$\begin{aligned}
Z_{V,Q}(t) = X_{V,Q}(0) &+ \frac{1}{\sqrt{V}}\sum_\ell \ell \int_0^t \beta^{1/2}_{\ell,Q}(Z_V(u))dW_{\ell,Q}(u) \\
&+ \frac{1}{\sqrt{V}}\int_0^t \left(-(\beta^+_{drag,Q}(Z_{V,Q}(u)))^{1/2} + (\beta^-_{drag,Q}(Z_{V,Q}(u)))^{1/2}\right) dW_{drag,Q}(u) \\
&+ \int_0^t \left(F_Q(Z_V(u)) - \beta^+_{\text{drag},Q}(Z_{V,Q}(u)) + \beta^-_{\text{drag},Q}(Z_{V,Q}(u))\right) du
\end{aligned}$$

Launch process for satellites can be also considered as a Poisson process with rate λ, as in Section 3.2. Satellite dynamics can be expressed as:

$$X_{V,S}(t) = X_{V,S}(0) + \sum_\ell \frac{1}{V}\ell Y_{\ell,S}\left(V\int_0^t \beta_{\ell,S}(X_V(u))du\right) + \frac{1}{V}Y_{\text{launch}}(V\lambda t)$$

Applying the same logic as the drag counterpart:

$$Z_{V,S}(t) = X_S(0) + \frac{1}{\sqrt{V}}\sum_\ell \ell\int_0^t \beta^{1/2}_{\ell,S}(Z_V(u))dW_{\ell,S}(u) + \int_0^t F_S(X(u))\,du + \frac{1}{\sqrt{V}}\int_0^t \sqrt{\lambda V}dW_{\text{launch},S}(u) + \int_0^t \lambda V du$$

5 Simulations

This section discusses a simulation of objects in Low Earth Orbit (LEO) using two different mathematical approaches:

- ODE (Ordinary Differential Equations): A deterministic approach that models the average, smooth evolution of the population in each shell.

- SDE (Stochastic Differential Equations): A stochastic approach that incorporates random fluctuations in the population, capturing more of the uncertainty and variability in object dynamics over time. For the simulation the SDEs are simulated by Euler-Maruyama algorithm.

The primary objective is to understand how the presence of stochastic effects impacts the mid-term evolution of species populations before scaling the volume. We observe the evolution of species populations by shell, which includes satellites, derelicts, and debris. These populations change over time due to collisions, satellite launches, and atmospheric drag.

In this simulation, we use a 3-shell example to examine the effects of stochasticity and the impact of volume scaling in smaller volumes of Low Earth Orbit (LEO) before scaling the model to larger volumes. We simulated the system for the lowermost 3 shells with equal volume of 1,000km^3 (3 shells being about $2m$ apart), representing different altitudes in LEO system. The simulations were run over a 10-year period. We assume that there are no objects coming from the upper shell due to the atmospheric drag in the highest shell. The launch rates are [0.0280155, 0.0280157, 0.0280161] launches per year for [Low, Middle, High] shell, respectively.

In smaller volumes, randomness would have a more significant impact on the system's behavior. The simulation allows us to see the raw effects of stochasticity before scaling to larger volumes. The main finding is that debris species began to take over the system in the Euler-Maruyama results, while in the ODE case, the populations evolved more smoothly with less pronounced debris accumulation. In this case, the SDE simulation demonstrates how randomness accumulates and affects the system.

Shown as in Figure 2, one of the main findings from the E-M simulations is that the debris species begins to dominate the system over time. On the other hand, in the ODE model, the debris population grows at a steady rate, the E-M results show a significant increase in the debris population compared to the ODE case. The randomness introduced by the E-M method accumulates over time, leading to large, abrupt increases in debris as random collisions generate more debris than expected. These stochastic events result in debris beginning to overwhelm the system, particularly in the later stages of the simulation.

We further ran 200 E-M simulations and averaged the results to compare the average paths of the SDEs to the ODE solution. The debris population in the stochastic case shows a much steeper increase than in the ODE model as shown in Figure 3. The averaged paths of the E-M simulations provide insight into how stochastic effects influence the long-term behavior of the system. The average debris population in the SDE case grows significantly faster than in the ODE case. This suggests that stochastic interactions between species can lead to higher debris generation than deterministic ODE model.

We averaged the species evolution by each shell. In Figure 4a, the yellow curve represents the lowest shell, green represents the middle shell, and the purple represents the highest shell. Here we can observe the population ordering of the shell. We observed that the lower shell has higher population and higher shell has lower population. The results are in line with the ordering in the ODE case but are distinguished in the SDE case.

The differences between the ODE and SDE solutions implies the importance of considering stochasticity when modeling complex systems like LEO object populations. The ODE model, while useful for capturing the overall trends and aggregate behavior, fails to account for the random events that have a significant impact on the population dynamics, particularly for debris.

We futher exteneded the analysis to over a 50-year, long time horizon, and averaged the sample paths. We aim to observe the long-term effects of stochasticity on debris accumulation and to identify any trends that could impact the long-term sustainability of Low Earth Orbit (LEO) operations. Extending the time horizon to 50 years provides more insight into the cumulative impact of random events and potential long-term risks.

Shown as in Figure 5, in the E-M simulations, the debris population appears to increase exponentially after a certain point. This is likely due to debris leading to more collisions, which generates even more debris, creating a feedback loop. By the end of the 50-year period, the debris population in the stochastic model is significantly larger than in the deterministic model, highlighting the long-term risks of runaway debris generation. The stochastic nature of the system causes some satellites to be destroyed much earlier than predicted by the ODE model, hindering the growth of the satellite population. Also, the stochastic model shows a higher accumulation of derelicts.

The SDE model suggests that debris accumulation could cause issues in the LEO system. As shown in its simulation, even small random fluctuations can lead to drastically different outcomes over time, making

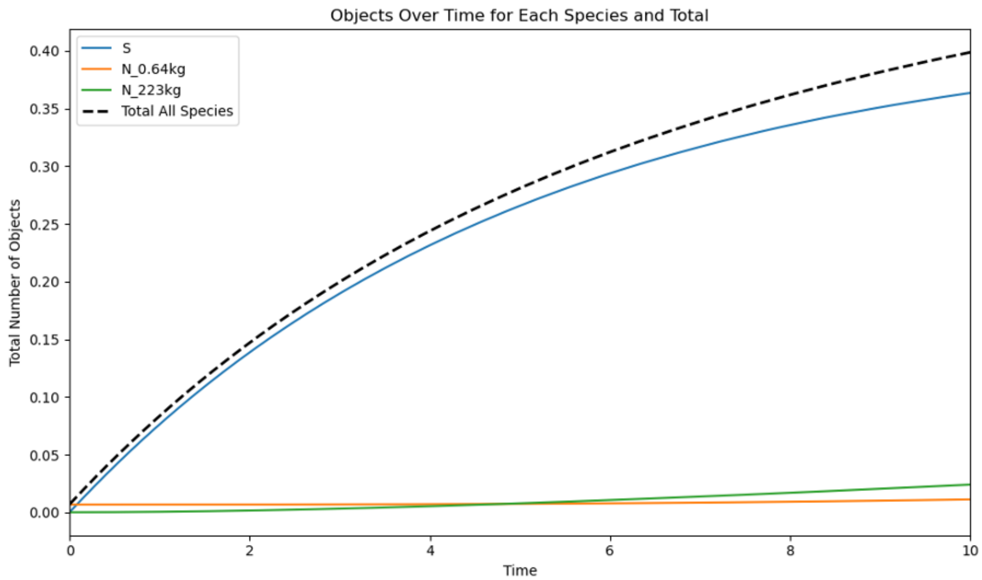

(a) ODE solutions for the 3-shell case.

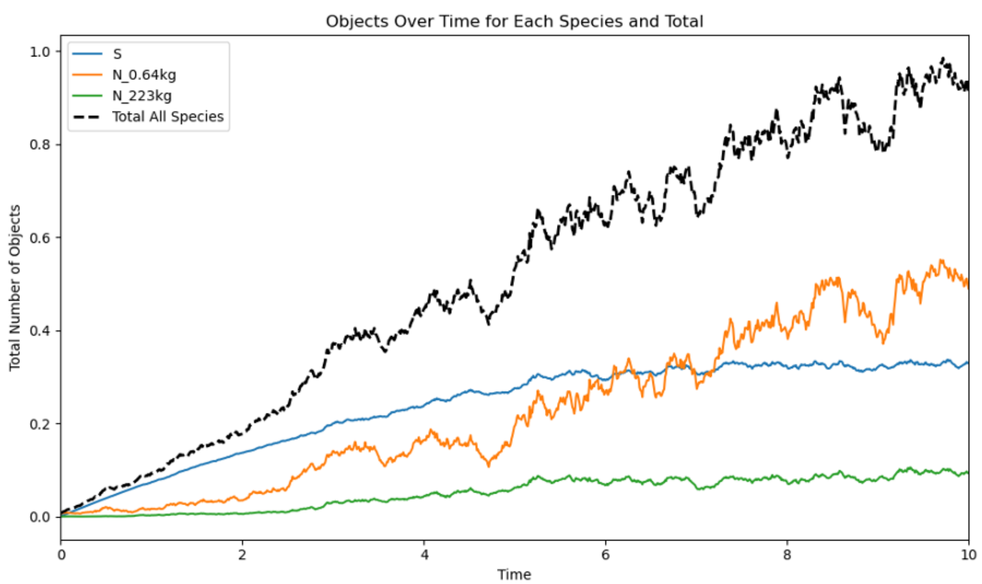

(b) SDE solutions for the 3-shell case.

Figure 2: Results of LEO evolution simulation of a simplified 3-shell model

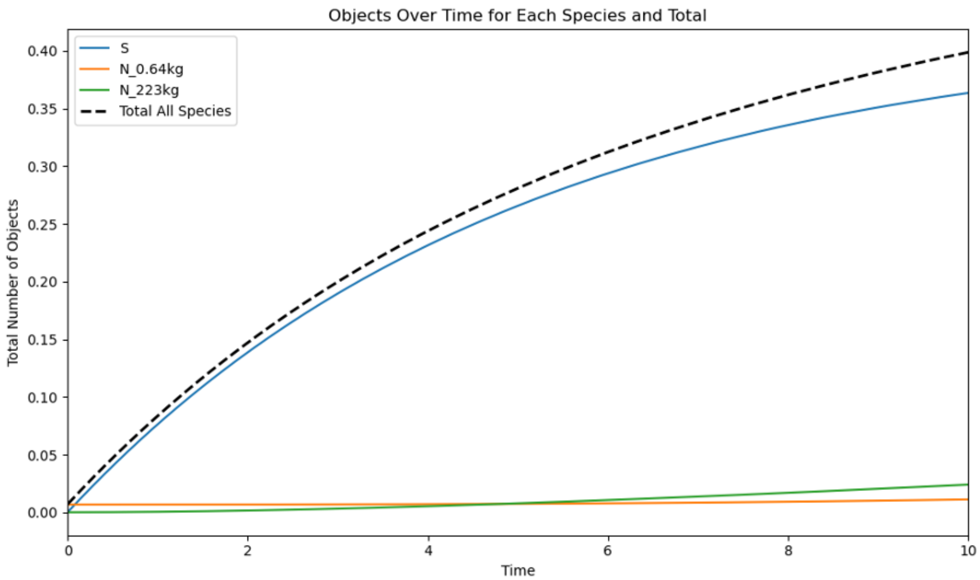

(a) ODE solutions for the 3-shell case.

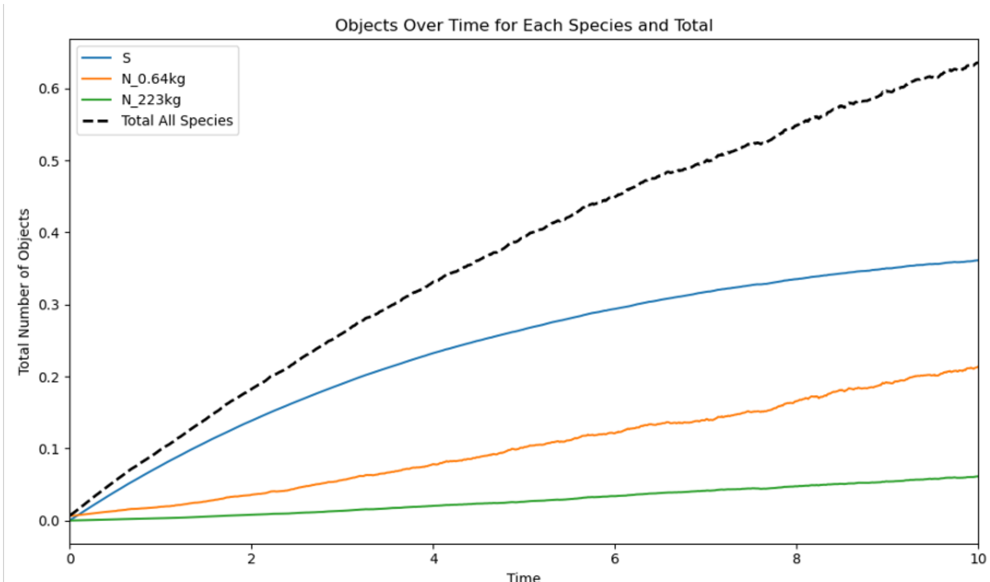

(b) SDE averaged solution paths for the 3-shell case.

Figure 3: Results of averaged LEO evolution simulation of a simplified 3-shell model

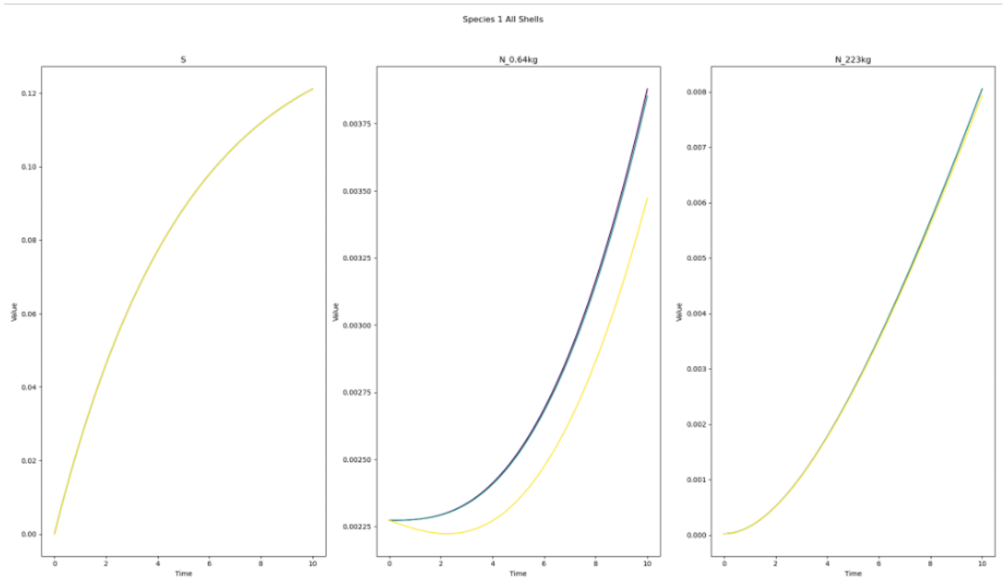

(a) ODE solutions: species by shell

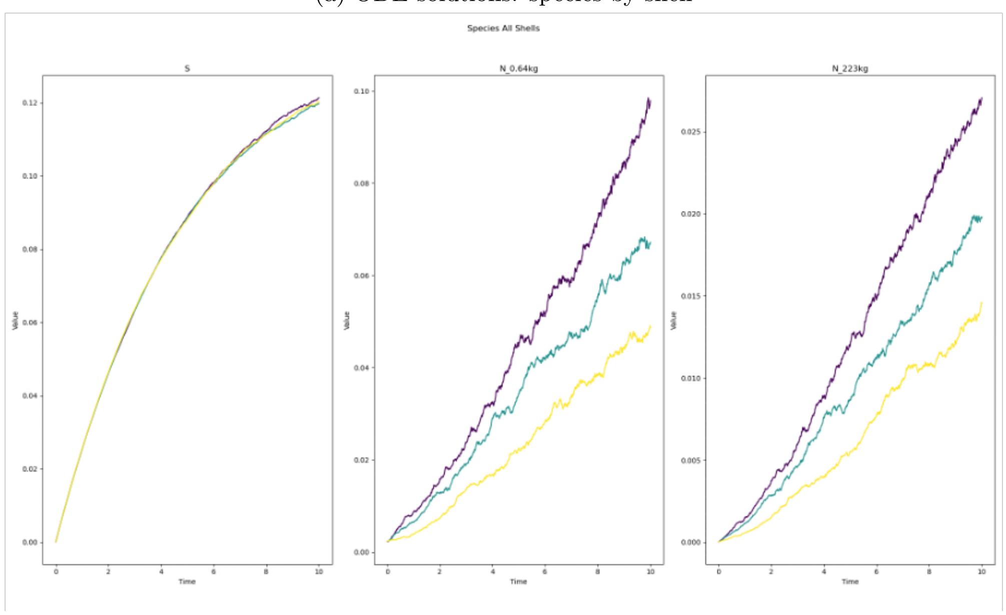

(b) SDE average path: species by shell

Figure 4: Results of averaged LEO evolution simulation: by species and shells

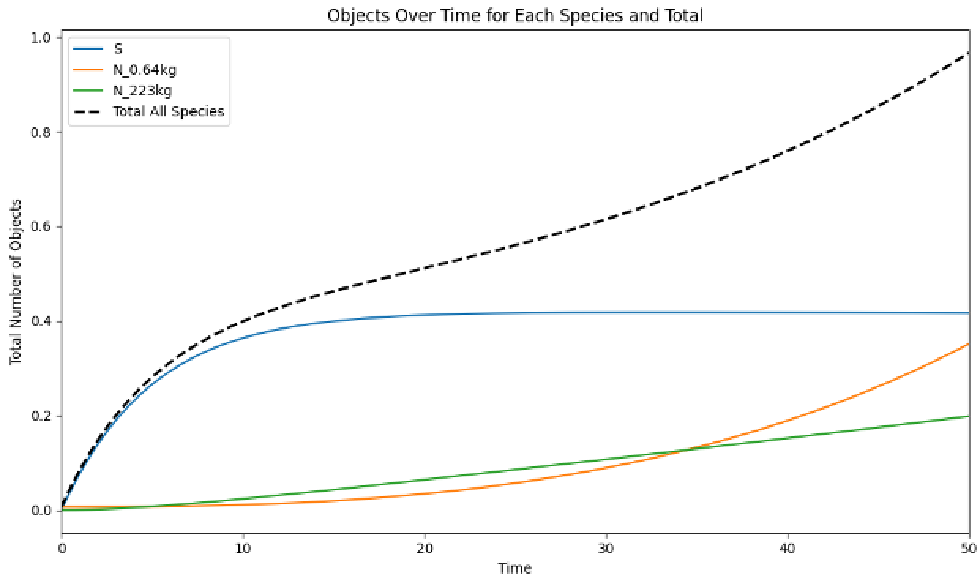

(a) ODE solutions for 50-year time horizon

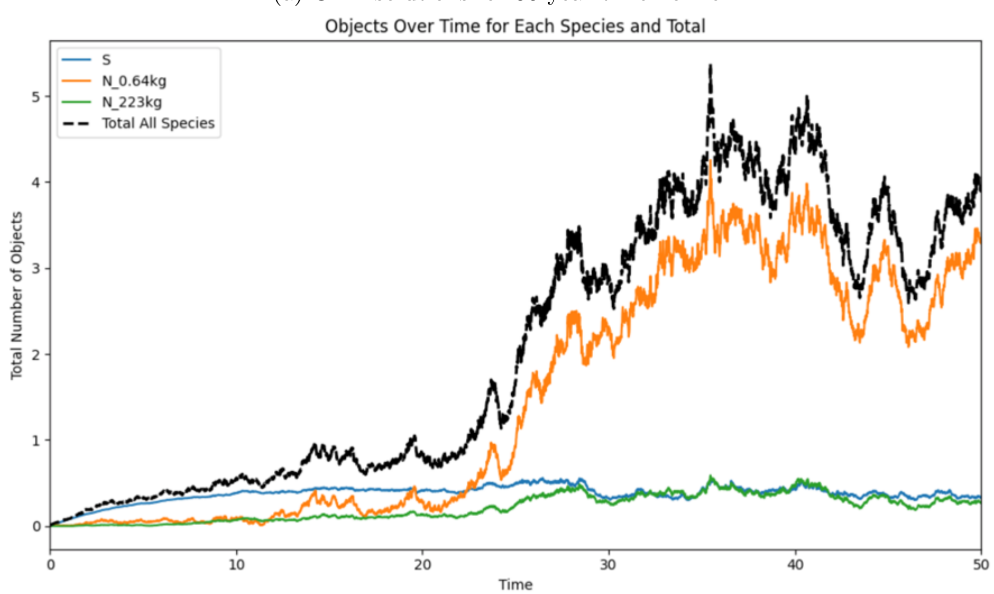

(b) SDE average path for 50-year time horizon

Figure 5: Long-Term Analysis of LEO Dynamics over a 50-Year Horizon

stochastic models essential for LEO system analysis. In the stochastic case, debris is more likely to dominate the system, which could lead to a runaway feedback loop where more debris results in further collisions, thus generating even more debris. This outcome is particularly concerning for long-term space sustainability and the potential for the Kessler Syndrome.

6 Conclusion

The results of this study suggests the importance of considering stochastic effects when modeling object dynamics in Low Earth Orbit system. While the deterministic ODE model provides insights into the average behavior of satellites, derelicts, and debris, it fails to capture the randomness of collisions and debris generation. The Stochastic Differential Equation (SDE) model, simulated using the Euler-Maruyama method, shows that randomness can significantly alter population trajectories, particularly with regard to debris accumulation.

References

D'Ambrosio, A., Lifson, M., and Linares, R. (2022). The capacity of low earth orbit computed using source-sink modeling. *arXiv preprint arXiv:2206.05345*.

Draief, M. and Massoulié, L. (2009). *Epidemics and Rumours in Complex Networks*. London Mathematical Society Lecture Note Series. Cambridge University Press.

D'Ambrosio, A., Servadio, S., Mun Siew, P., and Linares, R. (2023). Novel source–sink model for space environment evolution with orbit capacity assessment. *Journal of Spacecraft and Rockets*, 60(4):1112–1126.

Ethier, S. N. and Kurtz, T. G. (2009). *Markov processes: characterization and convergence*. John Wiley & Sons.

Long, G. et al. (2020). The impacts of large constellations of satellites.